Applied Catalysis A, General 718 (2026) 120892

Contents lists available at ScienceDirect

Applied Catalysis A, General

journal homepage: www.elsevier.com/locate/apcata

Dispersion assessment of $H_3PMo_{12}O_{40}$ supported on TiO_2 through *in situ* IR upon pyridine adsorption

ARTICLE INFO

Keywords:
FTIR spectroscopy
pyridine adsorption
Keggin heteropolyacids
dispersion
supported catalyst

ABSTRACT

Keggin heteropolyacids (HPAs) are powerful catalytic materials because of their particularly high acid strength. Dispersing them on a support is a commonly adopted strategy to overcome their low specific surface area and increase their recoverability. In this regard, their dispersion needs to be characterized. *In situ* IR measurements upon pyridine adsorption (IR-py) has recently been carried out on TiO_2-supported $H_3PW_{12}O_{40}$ to assess its dispersion quantitatively for the first time. Herein, we report the precautions to take when extending this approach to another Keggin HPA, namely $H_3PMo_{12}O_{40}$ (HPMo). In particular, the purpose of the current work is to comment on the earlier published work rather to present a full study and to show that, for reducible HPAs like $H_3PMo_{12}O_{40}$, reoxidation is required to employ IR-py as a tool to quantify dispersion. For these reasons, no catalytic tests are provided and the extent of reoxidation is not measured/characterized as well.

1. Introduction

The high Brönsted acidity of Keggin heteropolyacids (HPAs) – which have the formula $H_nXM_{12}O_{40}$ (X being generally P or Si and M being W or Mo) [1] – is often exploited to catalyze reactions requiring strong acidity [2,3]. Due to their low specific surface area in the solid state, HPAs are usually dispersed on a support aiming to harness the full potential of their catalytic effect.

However, the dispersion of Keggin HPAs is often not characterized precisely, likely because dedicated analytical tools are lacking or only give qualitative or semi-quantitative (*e.g.* XPS or PXRD [2]) information. Recently, the dispersion of $H_3PW_{12}O_{40}$ (HPW) on TiO_2 was quantitatively assessed through *in situ* IR pyridine (IR-py) adsorption measurements [4]. This method exploits the *pseudo*-liquid behavior of HPAs, which is described as being the absorption of a small polar molecule into the bulk of HPAs in the solid state [5,6]. When pyridine is absorbed into the bulk of HPW ("bulk" here refers to the inside of HPW crystals, not to the inside of a single HPW unit), a pyridinium salt is formed and its ν_{19b} vibration band around 1540 cm^{-1} (pyridinium ring stretch mode) is split in two [7,8]. This phenomenon is attributed to a tunneling effect caused by a frustrated in-plane pyridinium ring rotation in $(PyH)_3PW_{12}O_{40}$ [9] (Fig. 1). As this tunneling effect only takes place with bulk HPW, its uncommon IR-py spectrum can be used as a tool to discriminate well dispersed isolated HPW units at the surface of a support (without band splitting) from agglomerated ones (with band splitting). More importantly, by treating the spectrum properly (see ref. [4]), the fraction of well dispersed HPW units, hence their dispersion, can be quantified.

To our knowledge, IR-py has never been used to quantify the dispersion of other HPAs than HPW. Here we extend its implementation to $H_3PMo_{12}O_{40}$ (HPMo) supported on TiO_2 by showing under which conditions this approach can be used for reducible HPAs.

2. Experimental section

2.1. Materials

$H_3PMo_{12}O_{40}{\cdot}nH_2O$ (>99%) was purchased from Sigma-Aldrich. TiO_2 P25 was purchased from Degussa. Pyridine (anhydrous, 99.8%), ethanol (>99%) and O_2 (Alphagaz 1) were purchased from Aldrich, VWR Chemicals and Air Liquide, respectively. Silicon (100) wafers FZ (2 cm^2, 500 μm width, resistivity>10,000 Ω·cm) were purchased from Neyco (Vacuum & Materials).

2.2. Methods

2.2.1. Preparation of $H_3PMo_{12}O_{40}$ supported on TiO_2

To a 250 ML round-bottom flask containing 100 ML of ethanol, 1 g of support was suspended. The suspension was sonicated for 15 min. Then, a 20 ML ethanol solution containing a certain quantity (depending on the aimed loading) of dissolved $H_3PMo_{12}O_{40}{\cdot}6\,H_2O$ (dried under vacuum at <30 mbar and 25 °C beforehand to remove all physisorbed water) was added dropwise to the suspension. The mixture was then stirred for 2 h before removing the solvent with a rotary evaporator (40 °C, 280 rpm). The powder was recovered, crushed in a mortar and then further dried overnight at 25 °C under vacuum (<30 mbar). The aimed loading is expressed as %ML, *i.e.*, the theoretical amount of Keggin units required to cover a certain percentage of TiO_2 with one ideal monolayer (abbreviated as "ML"). We prepared samples with nominal loadings of 20, 50 and 80%ML.

An example of the calculation for supporting 10% ML of

Abbreviations: HPMo, phosphomolybdic acid $H_3PMo_{12}O_{40}$; HPW, phosphotungstic acid $H_3PW_{12}O_{40}$; % ML, percentage of the surface recovered by one ideal monolayer of Keggin units; IR-py, *in situ* infrared spectroscopy upon pyridine adsorption.

https://doi.org/10.1016/j.apcata.2026.120892
Received 4 March 2026; Accepted 9 March 2026
Available online 12 March 2026
0926-860X/© 2026 Elsevier B.V. All rights are reserved, including those for text and data mining, AI training, and similar technologies.

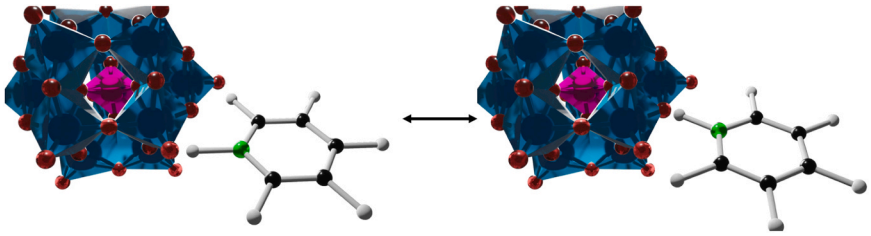


Fig. 1. In-plane pyridinium ring rotation in $(PyH)_3PW_{12}O_{40}$. Pink tetrahedron: PO_4. Blue octahedra: (WO_6). Red: oxygen atoms. Black: carbon atoms. White: hydrogen atoms. Green: nitrogen atom. LEFT: Hydrogen bonding between the NH of pyridine and edge-shared oxygen atom of HPW. RIGHT: Hydrogen bonding between the NH of pyridine and terminal oxygen atom of HPW.

$H_3PMo_{12}O_{40}{\cdot}6\,H_2O$ on 1 g of TiO_2 is provided hereunder:

The projected area of the single Keggin unit (S_K), approximated as a 1 nm-diameter (D) sphere is obtained as follows:

$$S_K = \frac{\pi D^2}{4} = \frac{\pi 10^{-18}}{4} = 7.85 \cdot 10^{-19}\ m^2$$

The number of Keggin anions (N_K) required to achieve a 10% ML coverage of 1 g of TiO_2 with a 50 m^2/g specific surface area (S_T) is given by:

$$N_K = ML \cdot \frac{S_T}{S_K} = 0.1 \cdot \frac{50}{7.85 \cdot 10^{-19}} = 6.37 \cdot 10^{18}$$

The mass of the sample (m_K) to be supported is:

$$m_K = \frac{N_K}{N_A} M_{W_K} = \frac{6.37 \cdot 10^{18}}{6.022 \cdot 10^{23}} \cdot 1933.48 = 20.4 \quad mg$$

with N_A the Avogadro number and M_{Wk} the molar mass of $H_3PMo_{12}O_{40}{\cdot}6\,H_2O$.

2.3. Characterizations

To assess the state of HPMo units on the different prepared materials via methods independent of the IR one we report here, XPS and XRD were used.

2.3.1. Inductively coupled plasma-atomic emission spectroscopy (ICP-AES)

The effective Mo loading on the different samples was measured by ICP-AES at the *Centre Terre et Pierre (CTP)* based in Antoing (Belgium). For this matter, each sample was mixed with 1 g of NaOH and Na_2O_2 and melted on the flame of a Bunsen burner. Melted samples were acidified with HCl and diluted with distilled water prior to analysis.

2.3.2. X-ray photoelectron spectroscopy (XPS)

The analyses were carried out with a SSX 100/206 photoelectron spectrometer from Surface Science Instruments (USA) equipped with a monochromatized micro focused Al X-ray source (powered at 20 mA and 10 kV). The sample powders pressed in small stainless-steel troughs of 4 mm diameter were placed on a ceramic carousel. The pressure in the analysis chamber was around 10^{-6} Pa. The angle between the surface normal and the axis of the analyzer lens was 55°. The analyzed area was approximately 1.4 mm^2 and the pass energy was set at 150 eV. In these conditions, the full width measured at half maximum (FWHM) of the Au 4 $f_{7/2}$ peak for a clean gold standard sample was about 1.6 eV. A flood gun set at 8 eV and a Ni grid placed above the sample surface were used for charge stabilization. The following sequence of spectra was recorded: survey spectrum, C 1 s, O 1 s, P 2p, Ti 2p, Mo 3p, Mo 3d and C 1 s again to check the stability of charge compensation with time. The aliphatic C-(C, H) component of the C 1 s peak of carbon was fixed to 284.8 eV to set the binding energy scale. Data treatment was performed with the CasaXPS program (Casa Software Ltd, UK). Some spectra were decomposed with the least squares fitting routine provided by the software with a Gaussian/Lorentzian (85/15) product function and after subtraction of a non-linear (Shirley) baseline. Molar fractions were calculated using peak areas normalized based on acquisition parameters and sensitivity factors provided by the manufacturer.

2.3.3. Powder X-ray diffraction (PXRD)

Diffractograms of the powder samples were recorded on a Bruker-D8 Advance diffractometer with a Bragg-Brentano geometry. A copper anode (Kα = 0.1548 nm) operated under 40 kV and 30 mA was used as X-ray source. The detector was a LynxEye XE-T. The angle (2θ) was varied from 5° to 80° at a speed of 5.93°/min (5051 steps of 0.015°). Well-grinded powders were dispersed on a "zero noise" sample holder coated with Vaseline® before insertion in the apparatus.

2.3.4. In situ Fourier transform infrared spectroscopy upon pyridine adsorption (IR-py)

Supported HPMo samples (about 20 mg) were pressed into 2 cm^2 self-supported wafers. As a self-supported wafer of bulk HPMo could not be made, a few ethanol droplets containing dissolved HPMo were deposited on a silicon wafer and then left to dry. The wafers were placed into a sample holder that was carefully transferred into a home-made IR cell equipped with KBr windows and connected to a vacuum line. All spectra (64 scans, 4 cm^{-1} resolution) were recorded at room temperature after pyridine adsorption upon evacuation under vacuum of the non-adsorbed pyridine moieties (10^{-6} Torr) on an Invenio spectrometer from Bruker equipped with a DTGS detector. Thermal treatments were carried out within a furnace at the top of the IR cell by moving the sample holder carefully with a magnet.

In a reference experiment, the sample was first evacuated (until reaching 10^{-6} Torr) at 100°C during 5 h. Then, it was cooled down to room temperature and exposed to 5 Torr of pyridine during 1 h, before being heated to 100°C for 1 h to further allow the diffusion of pyridine into the bulk of HPMo. The excess non-absorbed pyridine was then removed under vacuum, first at 100°C (1 h) and then at room temperature (1 h). Finally, the IR-py spectrum was measured.

As the drying step at 100 °C for 5 h was suspected to reduce $H_3PMo_{12}O_{40}$ into $H_3PMo^{VI}_{12-x}Mo^{V}_{x}O^{x-}_{40}$, the impact of a reoxidation step in-between the drying step and the adsorption of pyridine at room temperature was investigated. This reoxidation step was performed by submitting the sample to 100 Torr of O_2 at 120°C during 5 h.

3. Results and discussion

IR-py experiments were first carried out on bulk HPMo (Fig. 2a). In agreement with the literature [10,11], the spectrum "Without reoxidation" shows no splitting of the ν_{19b} band, in contrast to what was observed with HPW (Fig. 2b) [4]. IR-py experiments typically require an extensive drying of the HPA before pyridine adsorption. This step allows the removal of the structural water, ensuring a better interaction between the pyridine probe and the HPA. By performing this drying step under vacuum (10^{-6} Torr) and at 100°C, in the case of HPMo (which is reducible in contrast to HPW), it may inherently act as a reducing step. Hence, we hypothesized the reduction of $H_3PMo_{12}O_{40}$ to

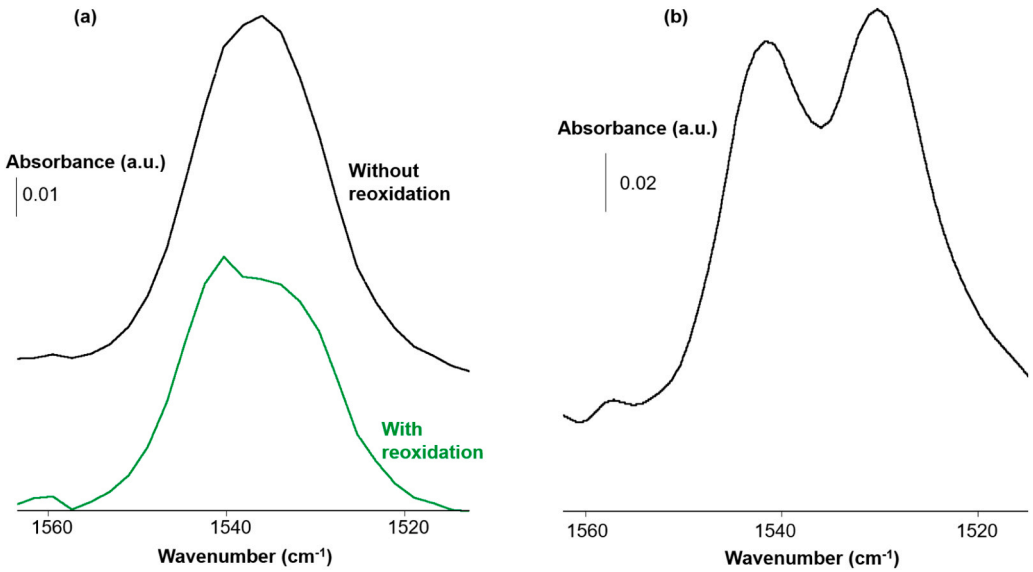


Fig. 2. FTIR spectra of (a) bulk HPMo after exposure to pyridine with and without a beforehand reoxidation step and (b) HPW after exposure to pyridine without a beforehand reoxidation step (reproduced from ref. [4]). For clarity, the spectra are restricted to the region around the ν_{19b} band. The Keggin structure was preserved and is shown on Fig. S1.

$H_3PMo^{VI}_{12-x}Mo^{V}_{x}O^{x-}_{40}$ species, which would lead to a decrease in the electrical charge of HPMo, in turn weakening its acid strength and thus its capability to adsorb the basic pyridine probe molecule. The occurrence of such reduction was confirmed indeed through a color change of the sample, shifting from yellow to blue [12]. To investigate whether this was the reason indeed for the disappearance of the ν_{19b} band splitting, HPMo was exposed to 100 Torr of O_2 at 120°C during 5 h after the drying step to reoxidize it and hence, to concomitantly restore its acid strength. Its resulting IR-py spectrum is the spectrum noted "With reoxidation" in Fig. 2a.

The ν_{19b} band splitting reappeared indeed on the spectrum "With reoxidation" but kept a lower extent of splitting than the equivalent band on the spectrum of the more strongly acidic HPW (Fig. 2b). These observations strongly suggest that the extent to which the ν_{19b} is split depends on the acid strength of the Keggin HPA. Indeed, the superior acid strength of HPW as compared to HPMo could explain why the splitting of the ν_{19b} band is more marked on the IR-py spectrum of HPW. The lower extent to which the ν_{19b} band is split in the case of HPMo could be explained by a partial reoxidation of HPMo too. Still, the ν_{19b} splitting was exclusively observed after reoxidation HPMo, hence with an increased acid strength, demonstrating that a greater acid strength of the Keggin HPA increases the extent to which the ν_{19b} band is split. The necessity of the reoxidation treatment in the case of HPMo compared to HPW can actually be attributed to its higher reducibility (HPMo has a reduction potential about 400 mV higher than HPW) [13,14], which leads to a decrease of its acid strength during the dehydration pre-treatment under vacuum at 100 °C prior to pyridine adsorption.

IR-py experiments with the reoxidation step were then carried out on HPMo/TiO_2 with different nominal loadings (20, 50 and 80% ML) (Fig. 3). ICP-AES measurements showed that the effective HPMo loadings for the three samples corresponded actually to 18, 47 and 74%ML (Table S1). XPS and PXRD analyses were also performed as qualitative references of the dispersion of HPMo (Fig. 4), without reoxidation step prior to analysis. The HPMo/TiO_2 spectra in Fig. 3 show an unsplit ν_{19b} band regardless of the HPMo loading. This result seems to contradict that observed by XPS (Fig. 4a). Indeed, from 0 to 60 ML%, the atomic Mo/Ti ratio increases linearly with the loading. Then, from 60 to 80 ML %, this ratio reaches a plateau at about Mo/Ti = 0.3. This deviation from linearity indicates the presence of agglomerated HPMo units at the surface of TiO_2 [2]. However, no splitting of the ν_{19b} band of pyridine

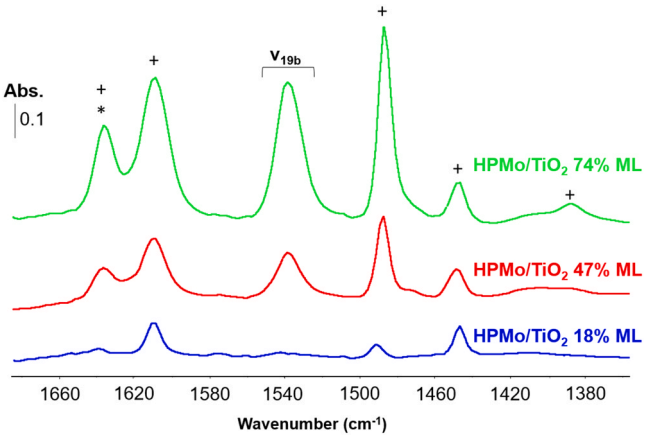


Fig. 3. FTIR spectra of HPMo/TiO_2 with different HPMo effective loadings after exposure to pyridine subsequent to a pre-treatment including a reoxidation step. The spectra are restricted to the region around the ν_{19b} band for clarity. At the exception of ν_{19b}, all bands are either specific to pyridine interacting with TiO_2 (marked with +) or to TiO_2 itself (marked with *) [4]. The Keggin structure was preserved and is shown in Fig. S2. Abs. = Absorbance (-).

could be detected by FTIR in this composition range. The non-detection of agglomerated HPMo units by both IR-py (Fig. 3) and PXRD (Fig. 4b) can be attributed to a smaller sensitivity of the two latter techniques. One could also wonder whether the reoxidation step, specific to the IR-py approach, could have increased the dispersion of HPMo on TiO_2, thereby decreasing the extent of the ν_{19b} band splitting, but this can be excluded as the Mo/Ti ratios measured by XPS before and after the reoxidation step were similar (Figure S3). Another likely explanation for the discrepancy between XPS without prior reoxidation and IR-py with prior reoxidation could be the fact that the reoxidation step was not sufficiently strong, leading to only partially reoxidized HPMo species and making the IR method not as sensitive as it could be.

4. Conclusion

In this study, we showed that the ν_{19b} band splitting is influenced not only by the dispersion of HPMo, but also by its acid strength. Indeed, the

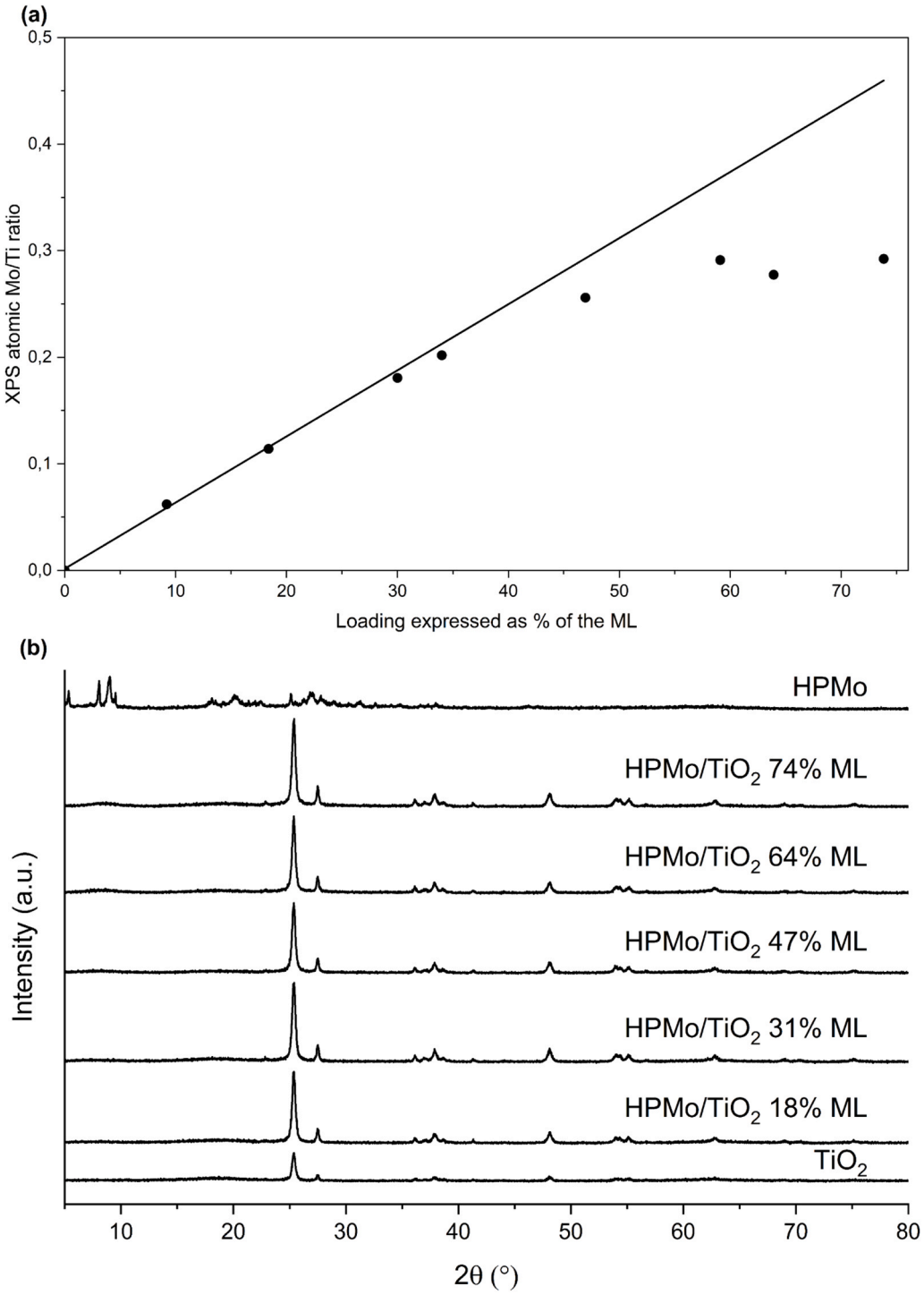


Fig. 4. (a) Mo/Ti atomic ratio at HPMo/TiO_2 surface measured by XPS *versus* HPMo effective loading (expressed as ML%) measured by ICP-AES. Black ● are experimental points while the black line is the line passing through the first two experimental points (0 and 10 ML%). (b) PXRD patterns of pristine TiO_2, HPMo/TiO_2 at different effective loadings, and bulk HPMo.

IR-py spectrum of reduced, consequently less acidic, HPMo exhibited an unsplit ν_{19b} peak which was however split once a reoxidation treatment was added in-between the dehydration pre-treatment under vacuum at 100 °C and the adsorption of pyridine. In the case of HPMo, XPS appeared to be more sensitive for detecting HPMo clusters than IR-py, whereas in the case of HPW, the opposite tendency was observed [4]. This discrepancy is attributed to the lower reducibility of HPW and its higher acid strength. Still, we believe that the sensitivity of IR-py on HPMo supported samples can be increased by optimizing the reoxidation prior to the pyridine adsorption step. Hence, in that case, IR-py could be a powerful tool to quantify the dispersion of reducible HPAs.

CRediT authorship contribution statement

Alexandre Vimont: Writing – review & editing. **Laetitia Valentin:** Data curation. **Eric M. Gaigneaux:** Supervision, Writing – review & editing. **Sophie Hermans:** Writing – review & editing. **Alixandre**

Magerat: Conceptualization, Data curation, Investigation, Writing – original draft. **Josefine Schnee:** Supervision, Writing – review & editing.

Declaration of Competing Interest

The authors declare that they have no known competing financial interests or personal relationships that could have appeared to influence the work reported in this paper.

Appendix A. Supporting information

Supplementary data associated with this article can be found in the online version at doi:10.1016/j.apcata.2026.120892.

Data availability

Data will be made available on request.

References

[1] C. Lang, J. Schnee, B.J. Takam Mba, F. Devred, E.M. Gaigneaux, Catal. Sci. Technol. 10 (2020) 6244–6256.
[2] J. Schnee, A. Eggermont, E.M. Gaigneaux, ACS Catal. 7 (2017) 4011–4017.
[3] R. Al-Faze, A. Finch, E.F. Kozhevnikova, I.V. Kozhevnikov, Appl. Catal. A Gen. 597 (2020) 117549.
[4] J. Schnee, F. Devred, E.M. Gaigneaux, A. Vimont, Appl. Catal. A Gen. 578 (2019) 116–121.
[5] R.M. Ladera, J.L.G. Fierro, M. Ojeda, S. Rojas, J. Catal. 312 (2014) 195–203.
[6] J. Schnee, E.M. Gaigneaux, Catal. Sci. Technol. 7 (2017) 817–830.
[7] A. Vimont, A. Travert, C. Binet, C. Pichon, P. Mialane, F. Sécheresse, J.-C. Lavalley, J. Catal. 241 (2006) 221–224.
[8] C. Pichon, P. Mialane, J. Marrot, C. Binet, A. Vimont, A. Travert, J.-C. Lavalley, Phys. Chem. Chem. Phys. 13 (2011) 322–327.
[9] C. Binet, A. Travert, M. Daturi, J.-C. Lavalley, A. Vimont, RSC Adv. 4 (2014) 19159–19164.
[10] N. Essayem, C. Lorentz, A. Tuel, Y.B. Tâarit, Catal. Commun. 6 (2005) 539–541.
[11] L. Mouheb, L. Dermeche, N. Essayem, C. Rabia, Catal. Lett. 150 (2020) 3327–3334.
[12] E.A. Nagul, I.D. McKelvie, P. Worsfold, S.D. Kolev, Anal. Chim. Acta 890 (2015) 60–82.
[13] J.J. Altenau, M.T. Pope, R.A. Prados, Hyunsoo So, Inorg. Chem. 14 (1975) 417–421.
[14] M.T. Pope, in: J.J. Borrás-Almenar, E. Coronado, A. Müller, M. Pope (Eds.), Polyoxometalate Molecular Science, Springer Netherlands, Dordrecht, 2003, pp. 3–31.

Alixandre Magerat*
Université catholique de Louvain (UCLouvain), Institute of Condensed Matter and Nanosciences (IMCN), - Molecular Chemistry, Materials and Catalysis (MOST), Place Louis Pasteur, 1 – box 04.01.09 1 or 04.01.034 – 1348, Louvain-la-Neuve, Belgium

Laetitia Valentin
Sorbonne Université, CNRS, Laboratoire de Réactivité de Surface, LRS, Paris F-75005, France

Alexandre Vimont
Université de Caen Normandie, ENSICAEN, CNRS, LCS, Laboratoire Catalyse et Spectrochimie, 14000 Caen, France

Sophie Hermans, Eric M. Gaigneaux
Université catholique de Louvain (UCLouvain), Institute of Condensed Matter and Nanosciences (IMCN), - Molecular Chemistry, Materials and Catalysis (MOST), Place Louis Pasteur, 1 – box 04.01.09 1 or 04.01.034 – 1348, Louvain-la-Neuve, Belgium

Josefine Schnee*
Sorbonne Université, CNRS, Laboratoire de Réactivité de Surface, LRS, Paris F-75005, France

* Corresponding author.

* Corresponding author.
E-mail addresses: alixandre.magerat@uclouvain.be, magerat.alixandre@gmail.com (A. Magerat).
E-mail address: josefine.schnee@sorbonne-universite.fr (J. Schnee).